A REDUCED BASIS FOR OPTION PRICING *

RAMA CONT †, NICOLAS LANTOS ‡, AND OLIVIER PIRONNEAU §

Abstract. We introduce a reduced basis method for the efficient numerical solution of partial integro-differential equations which arise in option pricing theory. Our method uses a basis of functions constructed from a sequence of Black-Scholes solutions with different volatilities. We show that this choice of basis leads to a sparse representation of option pricing functions, yielding an approximation whose precision is exponential in the number of basis functions. A Galerkin method using this basis for solving the pricing PDE is presented. Numerical tests based on the CEV diffusion model and the Merton jump diffusion model show that the method has better numerical performance relative to commonly used finite-difference and finite-element methods. We also compare our method with a numerical Proper Orthogonal Decomposition (POD). Finally, we show that this approach may be used advantageously for the calibration of local volatility functions.

Key words. Option pricing, PDE, PIDE, integro-differential equation, jump-diffusion, Merton model, Galerkin method, reduced basis.

AMS subject classifications. 37M25, 65N99

1. Introduction.

Option pricing problems can be formulated in terms of a partial differential (PDE) or integro-differential equation (PIDE) or inequality [1]. In a pricing model where the underlying asset follows a Markov process with infinitesimal generator $\mathcal{L}$, the (discounted) value $u(t, S)$ as a function of the date t and the underlying asset price S solves Kolmogorov's backward equation

$$\partial_t u(t, S) + \mathcal{L}u(t, S) = 0 \tag{1.1}$$

with appropriate boundary conditions which describe the payoff of the option. In the case of the Black-Scholes model, this pricing equation reduces to the Black-Scholes partial differential equation whose analytical solution leads to the famous Black-Scholes formula. When the random evolution of the underlying asset is driven by a Lévy process or more generally a time inhomogeneous jump-diffusion process, the operator $\mathcal{L}$ is an integro-differential operator, expressed as the sum of a second-order differential operator and an integral operator, and (1.1) becomes a partial integro-differential equation [7]. More generally, even when the evolution of underlying asset price is not Markovian, call options may be priced in terms of a *forward* PDE [9] or PIDE [2] involving integro-differential operators of the same type.

Except in the Black-Scholes model with constant volatility, solutions to such pricing equations are not known analytically in general and require numerical methods. A variety of techniques have been proposed to solve pricing equations. In special cases with constant coefficients, Fourier transform methods [5, 11] may be applied efficiently. More generally, finite difference and finite element methods have been used to solve the pricing P(I)DE [1, 7]. In models with jumps, the non local integral term leads to dense matrices after discretization [7] and efficient numerical methods are required for pricing of complex contracts and for calibration of model parameters.

Various techniques have been introduced to speed up the numerical solution of such pricing equations. In particular, for PIDEs with non-local terms, propositions include combining

*This research was partially supported by grants from the French Ministry of Research and Natixis.

†Laboratoire de Probabilités et Modèles Aléatoires, UMR 7599 CNRS-Université Pierre & Marie Curie, France & IEOR Dept, Columbia University, New York. (Rama.Cont@columbia.edu)

‡Université Pierre & Marie Curie, UMR CNRS 7598 Laboratoire Jacques Louis Lions, F-75252 Paris, France. & Natixis Corporate Solutions, 30 ave Georges V, 75008 Paris France (lantos@ann.jussieu.fr)

§Université Pierre & Marie Curie, UMR CNRS 7598 Laboratoire Jacques Louis Lions, F-75252 Paris, France (olivier.pironneau@upmc.fr)

Fourier methods with finite-difference approximations [3], splitting the operator into a differential and integral part and using an implicit-explicit time stepping [7] or compressing the operator using a wavelet basis representation [12].

A general idea, which underlies many numerical methods, is to project the solution of the pricing equation on a sequence of basis functions. In such projection methods, the choice of the basis functions is important for the numerical performance of such projection methods. In most existing approaches, the basis functions are chosen for analytical convenience –finite elements, wavelets– but may have little to do with the nature of the problem and may not take into account the shape of the solution or the specific boundary conditions which intervene in the pricing problem. In other cases, a basis is computed numerically for the problem at hand: this is the essence of the POD (Proper Orthogonal Decomposition) method [14, 16]. An important property of projection methods is whether the solution may be efficiently represented using a *small* number of basis functions, leading to small linear systems: this is the so-called *sparse representation* property.

In this work we propose a projection method which is adapted to the numerical solution of pricing equations such as (1.1). Our key idea is to construct a family of basis functions which is well suited for the pricing problem in the sense that solutions of the pricing equations will admit a sparse representation in this basis. Our construction is based on the observation that pricing functions, at a fixed date, are well approximated by a convex combination of (a few) Black-Scholes functions u_{σ_i} with different volatilities σ_i (see e.g. [4]). Since the pricing function u verifies (1.1), its evolution over a small time interval δt may be approximated as

$$u(.,(k+1)\delta t) - u(.,k\delta t) = -\delta t \mathcal{L} u(.,k\delta t) \tag{1.2}$$

So, intuitively, the *time increment* of the pricing function may be approximated by functions of the form $\mathcal{L}u_{\sigma_i}$, where u_{σ_i} are Black-Scholes pricing formulas. This suggests that functions of the form $\mathcal{L}u_{\sigma_i}$, where σ_i is an appropriately chosen sequence of volatility values, may be used to construct a sparse representation of solutions of the pricing equation (1.1). This intuition turns out to be correct: we will show that the images under the pricing operator of Black-Scholes pricing functions u_{σ_i} span a space of smooth functions decaying at infinity and that this space contains the solution of (1.1) (up to a translation) when a certain symmetry condition is verified (see Section 4). In the general case, we will show that one can complete this basis by adding twice as many functions constructed by a similar method.

We will explain this construction in more detail in Section 3 and show that it leads indeed, in many cases, to a sparse representation of pricing functions where less than 20 basis elements already yield an excellent precision for pricing purposes. In fact, we will show for the examples studied that the error decays exponentially with the number of basis functions. We then introduce a Galerkin method for solving the pricing equation (1.1) by projection on this *reduced basis*. By contrast with finite element or wavelet methods which lead to large, sparse matrices, our reduced basis method will lead to a numerical scheme involving small (less than 20×20) but full matrices. In addition, Black-Scholes pricing functions verifying the same boundary conditions as the solutions we want to approximate, such a representation will verify the right asymptotic properties at the boundaries: this approach gets rid of "numerical boundary conditions" or boundary adjustments at no further computational cost.

1.1. Outline. The paper is organized as follows. Section 2 introduces the problem and gives examples of PDEs and PIDEs in option pricing. In Section 3 we define the basis functions and show that they lead to a sparse representation for solutions of the pricing equation in the case of a diffusion model with general time- and price-dependent volatility and in a jump diffusion model with Gaussian jumps. The theoretical properties of the basis are studied in Section 4. In Section 5 we present a numerical scheme based on this reduced basis:

we discuss the numerical implementation and compare the results with a standard POD. The results in Section 5 show that the our reduced basis method

- is superior, in terms of precision per number of basis elements, with respect to standard numerically constructed reduced order models, and
- is 2 to 10 times faster than finite difference or finite element methods for pricing PDEs or PIDEs.

In particular, numerical tests in commonly used models show that using as few as 10 to 20 basis functions allows to reach a precision similar to that of finite difference methods typically used with 100 time steps and 200 mesh points in price. Section 6 shows an application of this method to the calibration of local volatility functions.

2. Partial integro-differential equations in option pricing. Many option pricing problems require efficient methods for solving a time dependent Partial Integro-Differential Equation (PIDE) of the following type

$$\partial_t w + \mathcal{L} w = f, \quad w(T) = \phi \tag{2.1}$$

where $\mathcal{L}$ is an integro-differential operator of Lévy type [6, 7, 12]. When the jumps in the underlying asset are driven by a Lévy process, the operator $\mathcal{L}$ is the sum of a convection-diffusion operator $\mathcal{L}^\sigma$ and an integral operator $\mathcal{L}_J$ representing the effect of jumps:

$$\begin{aligned}
\mathcal{L}^\sigma w(S,t) &= -\frac{1}{2}\sigma^2(S,t)S^2\partial_{SS}w(S,t) - (r-d)S\partial_S w(S,t) + rw(S,t) \\
\mathcal{L}_J w(S,t) &= -\int_{\mathbb{R}} \left[w(Se^z,t) - w(S,t) - S(e^z-1)\partial_S w(S,t)\right] J(z)dz
\end{aligned} \tag{2.2}$$

Popular models such as the variance Gamma model, the Merton model and the tempered stable model are obtained using various parametrizations for the Lévy kernel $J(z)$; for an overview of these and other models with jumps, see [6].

2.1. Change of variable. We introduce the following changes of variable:

$$\begin{aligned}
&\tau := T - t, \text{ the time to maturity.} \\
&y := e^{(r-d)(T-t)}\frac{S}{K}, \text{ the forward moneyness} \\
&x := \ln y \ \ (i.e.\ S = Ke^{x-(r-d)\tau}), \text{ the log forward moneyness (LFM),}
\end{aligned} \tag{2.3}$$

PROPOSITION 2.1. *Let $C \in C^{1,2}(\mathbb{R}\times[0,T],\mathbb{R}_+)$ be a solution of (2.1) with $f = 0$. Define*

$$\begin{aligned}
v(y,\tau) &:= \frac{e^{r\tau}}{K}C(yKe^{-(r-d)\tau}, T-\tau), \\
u(x,\tau) &:= v(e^x,\tau) = \frac{e^{r\tau}}{K}C(Ke^{x-(r-d)\tau}, T-\tau);
\end{aligned}$$

then

$$\begin{aligned}
&\partial_\tau v + \mathcal{L}^\sigma v + \mathcal{L}_J v = 0 \ \ \textit{in } \mathbb{R}^+\times(0,T), \ \ v(y,0) = v_0(y) := \phi(Ky) \\
&\partial_\tau u + \mathcal{L}^\sigma u + \mathcal{L}_J u = 0 \ \ \textit{in } \mathbb{R}\times(0,T), \ \ u(x,0) = u_0(x) := \phi(Ke^x)
\end{aligned}$$

where

$$\mathcal{L}^\sigma v(y,\tau) = -\frac{1}{2}\sigma^2 y^2 \partial_{yy} v$$

$$\mathcal{L}_J v(y,\tau) = \int_{\mathbb{R}} v(ye^z)J(z)dz - v(y)\int_{\mathbb{R}} J(z)dz - y\partial_y v(y)\int_{\mathbb{R}}(e^z-1)J(z)dz$$

in the forward moneyness variables and

$$\mathcal{L}^\sigma u(x,\tau) = \tfrac{1}{2}\sigma^2\partial_x u - \tfrac{1}{2}\sigma^2\partial_{xx}u$$
$$\mathcal{L}_J u(x,\tau) = \int_{\mathbb{R}} u(x+z)J(z)dz - u(x)\int_{\mathbb{R}} J(z)dz - \partial_x u(x)\int_{\mathbb{R}}(e^z-1)J(z)dz$$

in the log-forward moneyness variables.

2.2. Reduction to homogeneous initial conditions . In order to obtain a good asymptotic behaviour at infinity, we choose a *constant* volatility Σ and introduce

$$\pi(x,\tau) := u(x,\tau) - u_\Sigma(x,\tau), \tag{2.4}$$

where u_Σ is the Black-Scholes pricing function, solution of the problem

$$\partial_\tau u(x,\tau) + \mathcal{L}^\Sigma u(x,\tau) = 0, \;\; u(x,0) = u_0(x) \tag{2.5}$$

The equation for π has now a source term:

$$\begin{cases} \partial_\tau \pi(x,\tau) + \mathcal{L}^\sigma \pi(x,\tau) + \mathcal{L}_J \pi(x,\tau) = f(x,\tau) \\ \pi(x,0) = 0, \end{cases} \tag{2.6}$$

with $f(x,\tau) := -\partial_\tau u_\Sigma(x,\tau) - \mathcal{L}^\sigma u_\Sigma(x,\tau) - \mathcal{L}_J u_\Sigma(x,\tau)$.

2.3. Examples. In this we present three examples of commonly used models, which will be used in the numerical simulations. These models allow for semi-analytical solutions for specific options, which can then be used as a benchmark for assessing the accuracy of numerical schemes. However, the technique described in this paper are applicable to arbitrary jump-diffusion models, well beyond these examples.

2.3.1. Diffusion Models. The *Black-Scholes model* corresponds to σ constant and $\mathcal{L}_J = 0$. It has been extended to σ function of S and t. We shall refer to these as *diffusion models*. An example is the Constant Elasticity Variance (CEV) diffusion model, introduced by Cox [8], in which the volatility function σ in (2.5) is given by:

$$\sigma_{CEV}(x,\tau) := \alpha\left(Ke^{x-(r-d)\tau}\right)^\beta, \text{for some } \alpha > 0,\ \beta \leq 0 \tag{2.7}$$

The option pricing problem for π under the CEV diffusion model is then (2.6) with σ_{CEV} in $\mathcal{L}^\sigma$ and $\mathcal{L}_J = 0$; hence

$$f(x,\tau) = -\partial_\tau u_\Sigma(x,\tau) - \frac{1}{2}\sigma^2_{CEV}(x,\tau)\partial_x u_\Sigma(x,\tau) + \frac{1}{2}\sigma^2_{CEV}(x,\tau)\partial_{xx}u_\Sigma(x,\tau).$$

2.3.2. Merton model. In Merton's jump-diffusion model [13] the jump kernel J is given by a Gaussian kernel

$$J(z) = J_M(z) := \tfrac{\lambda}{\delta\sqrt{2\pi}}e^{-\frac{(z-\mu)^2}{2\delta^2}} \tag{2.8}$$

and the volatility function is assumed to be constant $\sigma(x,\tau) = \sigma_M$.

We obtain the associated problem for π under Merton's jump-diffusion model :

$$\begin{cases} \partial_\tau \pi(x,\tau) + \mathcal{L}^{\sigma_M} \pi(x,\tau) + \mathcal{L}_{J_M} \pi(x,\tau) = f(x,\tau) \\ \pi(x,0) = 0, \end{cases} \tag{2.9}$$

with $f(x,\tau) = -\partial_\tau u_\Sigma(x,\tau) - \mathcal{L}^{\sigma_M} u_\Sigma(x,\tau) - \mathcal{L}_{J_M} u_\Sigma(x,\tau)$.

3. A sparse representation for pricing functions. Projection methods, such as the Galerkin method, express the solution of the pricing equation in terms of a linear combination of certain basis functions. The choice of the basis functions is important for the numerical performance of such projection methods. In most existing approaches, the basis functions are chosen for analytical convenience but may have little to do with the nature of the problem and do not take into account the shape of the solution or the specific boundary conditions which intervene in the pricing problem. An important property of such a basis is whether the solution may be efficiently represented using a *small* number of basis functions: this is the so-called *sparse representation* property. In this section we construct a family of functions which is adapted to the pricing problem in the sense that solutions of the pricing equations will admit a sparse representation in this basis.

Solutions of the Black-Scholes equation with constant volatility have the following symmetry: $u\left(\frac{1}{y},\tau\right) = \frac{1}{y}u(y,\tau)$. It thus seems natural to work first with time and price dependent volatilities which yield similarly symmetric solutions. As we shall see, volatility functions which satisfy the following symmetry condition will play a special role:

$$\sigma(y,\tau) = \sigma\left(\frac{1}{y},\tau\right) \quad \forall y,\tau. \tag{3.1}$$

For *any* volatility function $\sigma : \mathbb{R}\times[0,T] \mapsto \mathbb{R}_+$, we can decompose σ^2 into a symmetric part and an antisymmetric part:

$$\sigma^2(y,\tau) = \underbrace{\frac{\sigma^2(y,\tau)+\sigma^2\left(\frac{1}{y},\tau\right)}{2}}_{\sigma_S^2} + \frac{\sigma^2(y,\tau)-\sigma^2\left(\frac{1}{y},\tau\right)}{2} \tag{3.2}$$

The corresponding Black-Scholes operator can be similarly decomposed as

$$\mathcal{L}^\sigma = \mathcal{L}^{\sigma_S} \underbrace{-\frac{\sigma^2(y,\tau)-\sigma^2\left(\frac{1}{y},\tau\right)}{2}\,\partial_{yy}}_{\mathcal{L}_A^\sigma} \tag{3.3}$$

3.1. Definition of basis functions. For a diffusion problem we introduce the following sequence of functions:

$$\begin{aligned} \omega_i(x) \;&= \omega_i^S(x) := \mathcal{L}^{\sigma_S}[u_{\sigma_i}](x,T) \qquad \forall i = 1,\dots,n \\ \omega_{i+n}(x) &= \omega_i^A(x) := \mathcal{L}_A^\sigma[u_{\sigma_i}](x,T) \qquad \forall i = 1,\dots,n \end{aligned} \tag{3.4}$$

where u_{σ_i} is the Black-Scholes solution with constant volatility σ_i, i.e. the solution of (2.5) with $\Sigma = \sigma_i$. To handle the case of models with jumps, we furthermore define

$$\begin{aligned} \omega_i(x) = \omega_i^S(x) &:= \mathcal{L}^{\sigma_M}[u_{\sigma_i}](x,T) \qquad \forall i = 1,\dots,n \\ \omega_{i+n}(x) = \omega_i^J(x) &:= \mathcal{L}_J[u_{\sigma_i}](x,T) \qquad \forall i = 1,\dots,n \end{aligned} \tag{3.5}$$

with the same notations. Note that the basis functions independent of time.

We denote by I the number of basis functions. In general $I = 2n$, except if (3.1) holds in which case $I = n$ as explained below.

REMARK 1. *As we shall see, it is not necessary to work with the decomposition* (3.2)-(3.3)*. If $\mathcal{L}_A^\sigma = 0$ then any symmetric σ will do in $\mathcal{L}^\sigma$, including a constant $\sigma_0 \notin \{\sigma_i, i \geq 1\}$.*

Similarly if $\mathcal{L}^\sigma_A \neq 0$ then ω_i^A may be defined with $\mathcal{L}^\sigma$ instead of $\mathcal{L}^\sigma_A$. This gives the following alternative basis in the case of CEV with σ defined by (2.7):

$$\begin{aligned} \omega_i(x) &= \omega_i^{BS}(x) := \mathcal{L}^{\sigma_0}[u_{\sigma_i}](x,T) \qquad \forall i = 1,\dots,n \\ \omega_{i+n}(x) &= \omega_i^{\sigma}(x) := \mathcal{L}^{\sigma}[u_{\sigma_i}](x,T) \qquad \forall i = 1,\dots,n. \end{aligned} \tag{3.6}$$

3.1.1. Evaluation of basis functions. With the notation $v_i = \sigma_i\sqrt{T}$, $\forall i = 1,\dots,n$ a straightforward computation leads to:

$$\omega_i^S(x) = -\frac{\sigma_S^2(x,T)}{2v_i}\frac{1}{\sqrt{2\pi}}e^{-\frac{1}{2}\left(\frac{x}{v_i}-\frac{v_i}{2}\right)^2} \qquad \omega_i^A(x) = -\frac{\sigma^2(x,T)-\sigma^2\left(\frac{1}{x},T\right)}{4v_i}\frac{1}{\sqrt{2\pi}}e^{-\frac{1}{2}\left(\frac{x}{v_i}-\frac{v_i}{2}\right)^2}.$$

The computation of $\omega_i^J(x)$ requires evaluating a convolution term $\int_{\mathbb{R}} u(x+z)J(z)dz$: efficient algorithm using fast Fourier transforms are available when the characteristic function of the log-price is known [5, 11].

PROPOSITION 3.1. *In the Merton model, we have the following expression for $\omega_i^J(x)$ basis function*

$$\omega_i^J(x) = \lambda\left(e^{x+\mu+\frac{\delta^2}{2}}\mathcal{N}(d_1) - \mathcal{N}(d_2) - u_{\sigma_i}(x,T) - \left[e^{\mu+\frac{\delta^2}{2}}-1\right]\partial_x u_{\sigma_i}(x,T)\right)$$

where $d_1 = \frac{x+\mu+\delta^2+\frac{v_i^2}{2}}{\sqrt{\delta^2+v_i^2}}$, $d_2 = \frac{x+\mu-\frac{v_i^2}{2}}{\sqrt{\delta^2+v_i^2}}$,

$$\text{with } \mathcal{N}(y) := \frac{1}{\sqrt{2\pi}}\int_{-\infty}^{y} e^{-\frac{t^2}{2}}dt. \tag{3.7}$$

The proof is given in appendix A.

3.1.2. Examples. In this section we plot the basis functions associated to call options in various models: Black-Scholes with constant volatility (B-S), the Constant Elasticity of Variance (CEV) diffusion model and the Merton jump-diffusion model. In these examples u_{σ_i} is the Black-Scholes formula for a call option with strike $K = 42$, where σ_i spans the following range of volatilities:

$$\{\sigma_i\}_{i=1..5} = 0.070, 0.124, 0.221, 0.393, 0.7 \tag{3.8}$$

The spot price is $S_0 = 40$, the continuous risk-free interest rate is 10% and the dividend yield is 2%. We choose $\sigma_0 = 0.15$. For CEV diffusion model we use $\beta = -0.3$ and $\alpha = \sigma_0 K^{-\beta}$. Merton parameters for the Lévy density function are $\lambda = 0.4$, $\mu = 0.5$ and $\delta = 0.6$ and $\sigma_M = \sigma_0$. Note that $\mu \neq \frac{\delta^2}{2}$ (see Proposition 4.6).

The B-S basis (respectively CEV and Merton) functions are plotted in Fig. 3.1 (respectively in Fig. 3.2 and in Fig. 3.3).

The basis functions decay exponentially to zero at infinity.

3.2. Sparse representation property. In the CEV diffusion model and the Merton jump-diffusion model the pricing function for call options has a semi-analytical solution see [17, 13]. We can thus test whether this exact solution is well represented by a linear combination of a few basis functions, and whether this representation is accurate enough for applications by projecting this exact solution $\pi(x,\tau)$ on the basis $\{\omega_i\}_{i=1,..,I}$.

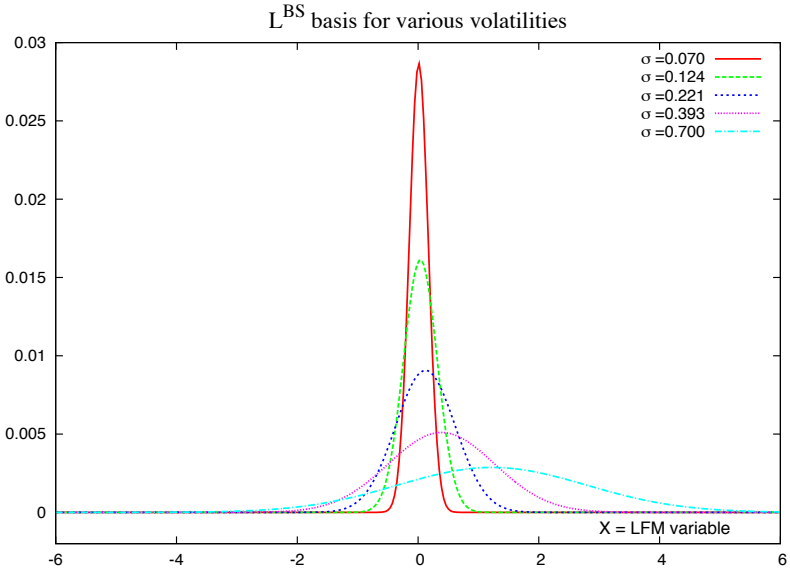

FIG. 3.1. *Plots of ω_i^{BS} for a call option with the 5 σ_i defined in (3.8) versus x, the Log Forward Moneyness (LFM) variable.*

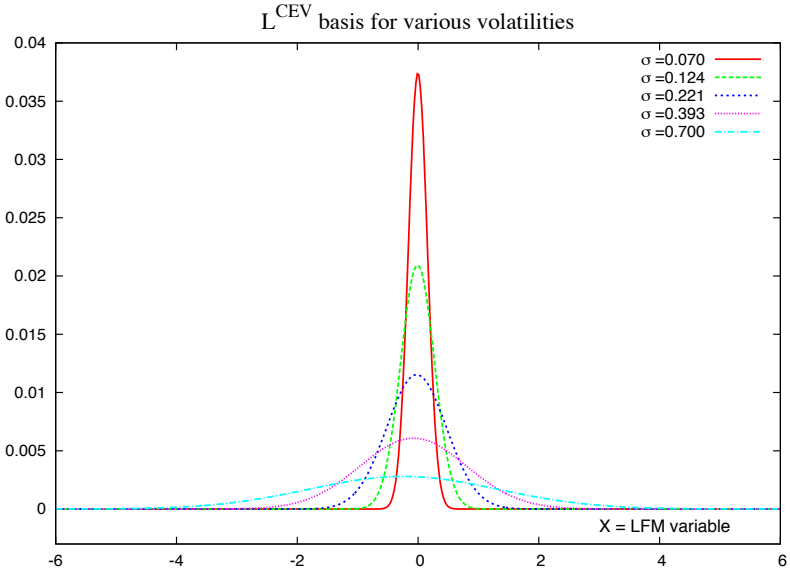

FIG. 3.2. *Plots of ω_i^{CEV} for a call option with the 5 σ_i defined in (3.8) versus x, the Log Forward Moneyness (LFM) variable.*

To numerically compute this projection, we build the Gram matrix for the L^2-scalar product and solve the associated linear system with GMRES; we have also tested SVD (using `svdcmp.c` of Numerical Recipes in C [15] and a least square solver using SVD, `dgelss.c` of LAPACK); While GMRES is usually faster, it is actually safer to use SVD so as to avoid a loss of precision for high values of I. Nevertheless, the results displayed here are obtained

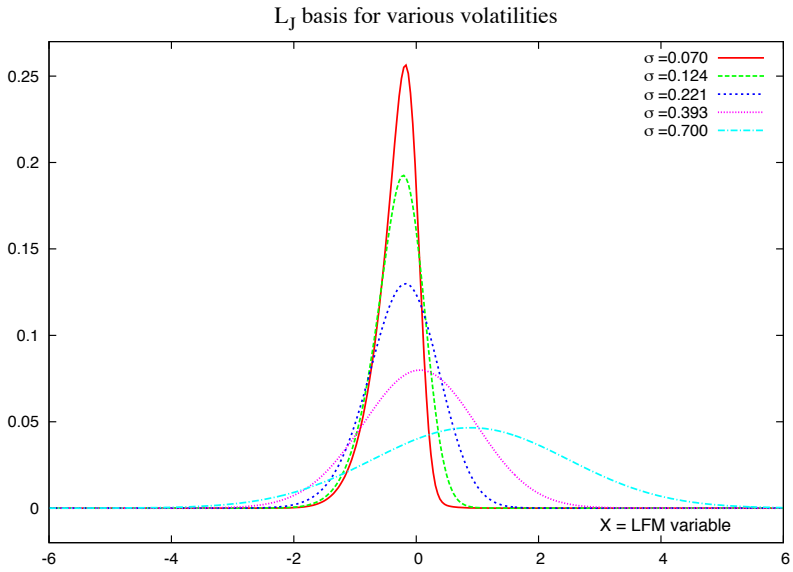

FIG. 3.3. *Plots of ω_i^J for a call option with the 5 σ_i defined in (3.8) versus x, the Log Forward Moneyness (LFM) variable.*

with GMRES.

We define Ω the finite computational domain for numerical integration and Ω_ϵ is a small domain around spot price where errors are computed. Ω_ϵ is defined as $[spot.e^{-\sigma_m\sqrt{T}}, spot.e^{\sigma_m\sqrt{T}}]$ for $\sigma_m = 0.15$ in the CEV case and $\sigma_m = \sqrt{\sigma^2 + \lambda(\mu^2+\delta^2)} = 0.5162$ in the Merton model.

To study the accuracy of the projection we plot for both models the L^2 relative pricing error:

$$\epsilon_p(\tau) = \frac{\int_{\Omega_\epsilon}[\pi_I(x,\tau)-\pi(x,\tau)]^2dx}{\int_{\Omega_\epsilon}[\pi(x,\tau)]^2dx} \tag{3.9}$$

expressed in percentage (%), as function of n. The σ_i are distributed in the segment $[\Sigma_{min}, \Sigma]$ according to the inverse of the square root (see Proposition 4.1. For the CEV model, we choose $\Sigma_{min} = 0.03$ and $\Sigma = 0.3$. The results obtained are shown in Fig. 3.4.

For Merton model, $2n$ basis functions are defined as in (3.5) with $\sigma = \sigma_0$, $\Sigma_{min} = 0.07$ and $\Sigma = 0.7$ are arbitrary chosen. The results are shown in Fig. 3.5.

In both cases the basis is observed to yield a sparse representation: the accuracy grows rapidly with the size of the basis n, allowing to retain a small number of basis functions in practice.

4. Basis property. We now proceed to show that the family of functions constructed above is indeed sufficient to represent any solution of the pricing equation (2.1).

4.1. The basis for diffusion operator.

4.1.1. Convergence. We choose to work with calls and with the formulation using the forward moneyness y and time-to-maturity τ. The basis functions are solutions at time $\tau = T$

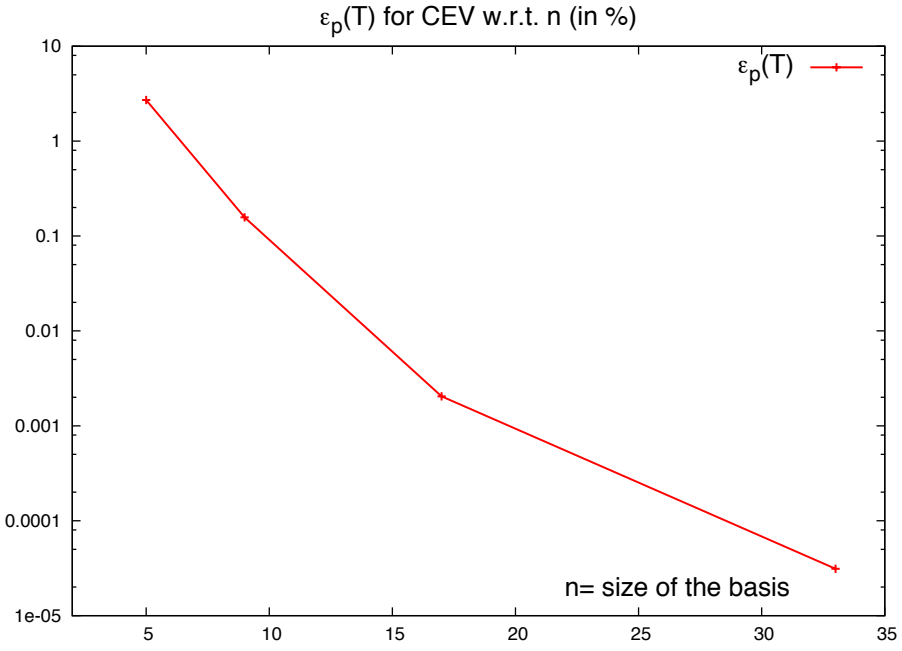

FIG. 3.4. *The projection error $\epsilon_p(T)$ (see equation 3.9) expressed in % and plotted in log scale for a call option under CEV volatility model w.r.t. the size of the basis $n = I/2$. The error is computed on $\Omega_\epsilon = [28.6, 56]$.*

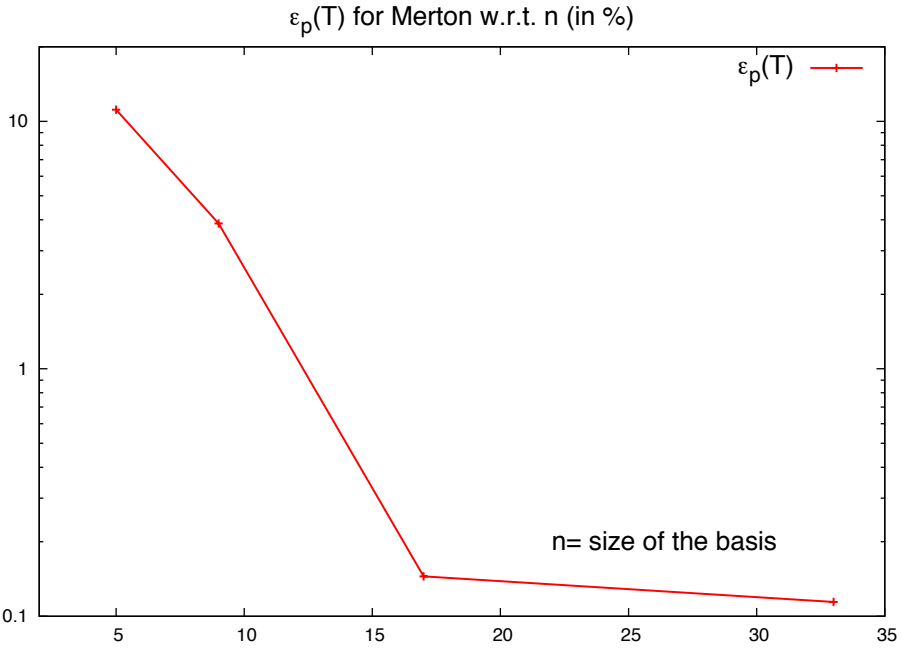

FIG. 3.5. *The projection error $\epsilon_p(T)$ (see equation 3.9) expressed in % and plotted in log scale for a call option under Merton model w.r.t. the size of the basis $n = I/2$. The error is computed on $\Omega_\epsilon = [12.6, 127]$.*

of

$$\partial_\tau v - \frac{\sigma^2 y^2}{2}\partial_{yy} v = 0, \text{ in } R \times [0,T], \;\; v(y,0) = (y-1)^+$$

for some σ. Using the well known analytical solution of the Black-Scholes equation with constant volatility σ_i:

$$\begin{aligned} v &:= \tfrac{e^{r\tau}}{K} Call(S,K,\sigma_i,t,T) \\ &= \tfrac{e^{r\tau}}{K}\left[S\mathcal{N}\left(\tfrac{\ln y}{\sigma_i\sqrt{\tau}} + \tfrac{\sigma_i\sqrt{\tau}}{2}\right) - Ke^{-r(T-t)}\mathcal{N}\left(\tfrac{\ln y}{\sigma_i\sqrt{\tau}} - \tfrac{\sigma_i\sqrt{\tau}}{2}\right)\right] \\ &= \tfrac{1}{2}\left(y\left[1 - \text{erf}\left(-\tfrac{\ln y}{\sigma_i\sqrt{2\tau}} - \tfrac{\sigma_i\sqrt{\tau}}{2\sqrt{2}}\right)\right] - 1 - \text{erf}\left(\tfrac{\ln y}{\sigma_i\sqrt{2\tau}} - \tfrac{\sigma_i\sqrt{\tau}}{2\sqrt{2}}\right)\right) \end{aligned}$$

Therefore

$$\begin{aligned} \mathcal{L}^\sigma v &:= -\frac{\sigma^2(y,T)y^2}{2}\partial_{yy} v \\ &= -\tfrac{\sigma^2(y,T)}{\sqrt{2\pi}2\sigma_i\sqrt{\tau}} e^{-\frac{1}{2}\left[\frac{\ln^2 y}{\sigma_i^2\tau} - \ln y + \frac{\sigma_i^2\tau}{4}\right]} = C_0\, \sigma^2(y,T)\sqrt{y} e^{-\frac{\ln^2 y}{2\sigma_i^2\tau}} \end{aligned} \tag{4.1}$$

where $C_0 = -\frac{e^{-\frac{1}{8}\sigma_i^2\tau}}{\sqrt{2\pi}2\sigma_i\sqrt{\tau}}$ does not depend on y.

REMARK 2. *Notice that $\sigma^{-2}(y,T)y^{-1/2}\mathcal{L}^\sigma v$ is an even function of $\ln y$. Accordingly, functions which do not have this symmetry cannot be written as a linear combination of $\mathcal{L}^\sigma v_{\sigma_i}$.*

PROPOSITION 4.1. *Consider the set of constant volatilities $\sigma_i = i^{-1/2}c,\ i = 1,2,3...$ for some real $c > 0$. Let v_i be the Black-Scholes Call at time T with constant volatility σ_i and let $\omega_i = \mathcal{L}^\sigma v_i$; Then $\{\omega_i\}$ is a basis for the set of continuous functions $f : \mathbb{R}^+ \to \mathbb{R}$ which decay exponentially fast at $+\infty$ and are such that*

$$f\left(\frac{1}{y}\right) = f(y)\frac{\sigma^2(y,T)}{y\sigma^2\left(\frac{1}{y},T\right)} \;\; \forall y > 0.$$

Proof. : According to (4.1), ω_i is proportional to $\sqrt{y}\sigma^2(y,T)e^{-i\frac{(\ln y)^2}{2c^2T}}$. Let $z = \frac{y}{y+1}$ and set

$$\varphi(z) = \exp(-\tfrac{1}{2c^2T}(\ln\frac{z}{1-z})^2),\ z \in [\frac{1}{2},1].$$

Consider the algebra generated by $\{\varphi(z)^i\}_{i=1,2..}$; by the Stone-Weiestrass theorem it is a basis for the continuous functions on $[\frac{1}{2},1]$ which are zero at $\frac{1}{2}$ and 1, because $z \to \varphi(z)$ is a separating function on $[\frac{1}{2},1]$ (i.e. $\varphi(z) \neq \varphi(z')$ for all $z \neq z' \in (\frac{1}{2},1)$). Given a function $y \to f(y)$; its corresponding function $z \to f(\frac{z}{1-z})$ can be written on the basis $\varphi^i(z)$, therefore:

$$f(y) = \sum_{i=1,2..} f_i\varphi(\frac{y}{1+y}),\;\; \forall y \in [1,+\infty)$$

If f has a symmetry about $y = 1$ the decomposition can be extended to $y \in [0, 1]$. Hence if $g(x)$ is even in $\ln y$ (i.e. $g(-\ln y) = g(\ln y)$), we decompose $g(\ln y) := f(y)\sigma^{-2}(y, T)/\sqrt{y}$ on the basis ω_i; this corresponds to the following restriction on f:

$$yf\left(\frac{1}{y}\right) = f(y) \tag{4.2}$$

□

PROPOSITION 4.2. *If $\sigma(y, \tau) = \sigma\left(\frac{1}{y}, \tau\right)$ and $f(y, \tau) = yf\left(\frac{1}{y}, \tau\right)$ for all $y > 0$ then the solution of*

$$\partial_\tau v - \frac{\sigma^2(y, \tau)y^2}{2}\partial_{yy}v = f, \;\; v(y, 0) = 0, \; \textit{in } \mathbb{R}^+ \times [0, T] \tag{4.3}$$

is invariant under the transformation $v(y) \to y\, v\left(\frac{1}{y}\right)$.

Proof. : Let us prove that $yv\left(\frac{1}{y}, \tau\right)$ satisfies the PDE when v does. Let $w(y, \tau) := yv\left(\frac{1}{y}, \tau\right)$. Notice that

$$\partial_{yy}w(y, \tau) = \frac{1}{y^3}\partial_{zz}v(z, \tau)|_{z=\frac{1}{y}}.$$

Therefore

$$\frac{1}{y}\partial_\tau w = \partial_\tau v\left(\frac{1}{y}, \tau\right) = \frac{\sigma^2\left(\frac{1}{y}, \tau\right)}{2y^2}\partial_{zz}v(z, \tau)|_{z=\frac{1}{y}} = \frac{\sigma^2(y, \tau)y^2}{2}\partial_{yy}w(y, \tau)$$

which means that w verifies also the PDE. Equation (4.2) differentiated at $y = 1$ gives $f(1) = 2f'(1)$, therefore if v^+ is the unique solution of (4.3) on $[1, \infty)$ and v^- is constructed from v^+ on $[0, 1]$ by (4.2), then $v^{+\prime}(1) = v^{-\prime}(1)$ and so $v^\pm$ is the unique solution of (4.3)on $\mathbb{R}^+$. □

Consequently, we have the following result:

THEOREM 4.3. *Let u_σ be the solution the pricing equation (2.1) without jumps ($\mathcal{L}_J = 0$) with a non constant volatility $\sigma(S, t)$ satisfying the symmetry condition*

$$\sigma(S, t) = \sigma(\frac{K^2}{S}e^{-2(r-d)(T-t)}, t), \;\; \forall y > 0, t \in (0, T) \tag{4.4}$$

Let Σ, c be real positive numbers and $\sigma_i = c/\sqrt{i}$. Let u_Σ, u_{σ_i} be the solutions of the Black-Scholes equation (2.5) with the corresponding volatilities. Then

$$u_\sigma(x, \tau) = u_\Sigma(x, \tau) + \sum_{i=1}^{\infty} \alpha_i(\tau)\mathcal{L}^\sigma u_{\sigma_i}(x, T) \tag{4.5}$$

for some time dependent but x-independent α_i.

Proof. : The data f and σ have the properties required by Proposition 4.2, so $u_\sigma - u_\Sigma$ can be decomposed on the basis $\{w^i\}$. □

THEOREM 4.4. *Assume that σ satisfies the symmetry property 4.4. Let $z = e^{-\frac{x^2}{2c^2T}}$; assume that in some interval $[x_m, x_M]$ all derivatives $\partial_z^i\sigma$ and $\partial_z^i u_\sigma$ are bounded, $i = 1, \ldots, I$. Then the projection error*

$$u_\Sigma(x, \tau) + \sum_{i=1}^{I} \alpha_i(\tau)\mathcal{L}^\sigma u_{\sigma_i}(x, T) - u_\sigma(x, \tau) \tag{4.6}$$

decays to zero exponentially in I near all x, τ where all derivatives of u_σ and u_Σ are uniformly bounded.

Proof. : Let $z = \exp(-x^2/(2c^2T))$, (see Proposition (4.1)), fix the time τ and consider $f(z) = (u_\sigma(x,\tau) - u_\Sigma(x,\tau))e^{-x/2}/\sigma^2$, with $\sigma = \sigma(x,T)$.

Then according to (4.1)

$$f(z) = \sum_{i=1}^{\infty} \alpha_i(\tau) z^i$$

Note that by comparison with a Taylor expansion this shows that $\alpha_i(\tau) = f^{(i)}(0)/i!$. Exponential convergence of $u_I \to u_\sigma$ will hold if $f^{(i)}(0)$ is bounded uniformly in i. This is difficult to prove directly because $z = 0$ corresponds to $x = \pm\infty$, i.e. $S = 0$ or $+\infty$. On the other hand we also know that, for any $z_0 \in (0,1)$, if the $f^{(i)}(z_0)$ are uniformly bounded

$$f(z) = \sum_{i=0}^{\infty} \frac{f^{(i)}(z_0)}{i!}(z - z_0)^i$$

This gives another expression for the α_i where its exponential decay is clearly seen:

$$\alpha_j = \sum_{i=j}^{\infty} C_i^j \frac{f^{(i)}(z_0)}{i!}(-z_0)^{i-j} = \sum_{p\geq 0}^{\infty} \frac{f^{(j+p)}(z_0)}{p!j!}(-z_0)^p \;\Rightarrow\; |\alpha_j| \leq \frac{e^{-z_0}}{j!} \max_i |f^{(i)}(z_0)|$$

This proves exponential convergence of the interpolation error of the exact solution at all points where all the derivatives of u_σ and u_Σ are bounded. To prove that the numerical approximation computed by the Galerkin method, has the same property we use the coercivity of the bilinear form of the Black-Scholes PDE and recall that in the H^1 norm the computed error is less than the interpolation error, up to a multiplicative constant. □

REMARK 3. *To prove differentiability with respect to z of u_σ the easiest is to write the PDE in this variable:*

$$\begin{aligned} &\partial_\tau v - 2\partial_z(\sigma^2 z^2 \ln\frac{1}{z}\partial_z v) + \beta z \partial_z v = f, \\ &\text{with } \beta = 2z\ln\frac{1}{z}\partial_z\sigma^2 + \sigma^2(\sqrt{\ln\frac{1}{z}} - 1 + 2\ln\frac{1}{z}) \end{aligned} \tag{4.7}$$

Variational methods with Sobolev weighted norms (as in [1]) shows that the solution exists with the regularity of f plus 2 except at $z = 0$ and $z = 1$ the Strike). When symmetry does not hold, the PDE must be studied by different methods on $y \in (0,1)$ and $y \in (1,\infty)$ and patched at $y = 1$. It is very likely that the regularity holds also but since the problem is not standard; a detailed study will be done separately.

REMARK 4. *For the pricing equation (2.1) with non constant volatility with symmetry and no jump, any symmetric σ can be used to construct the basis, not just $\mathcal{L}^\sigma$. This justifies the alternative use of a constant vol σ_0 in Remark 1. Once this is done the remaining basis vector can be any family of independent vectors, either $\mathcal{L}^{\sigma_{CEV}} u_{\sigma_i}$ or $\mathcal{L}^\sigma{}_A u_{\sigma_i}$.*

4.1.2. Numerical Validation. In this section, we check numerically the importance of the symmetry condition in the volatility. To this purpose we consider a *Gaussian volatility* (GV) model with $\sigma(x,\tau) = e^{-0.1x^2}$. On a call option , we choose to compare $\epsilon_p(T)$, the relative error introduced in 3.9) for 3 cases: **1)** the Black-Scholes model, **2)** Gaussian volatility model which both verify the symmetry condition and **3)** the CEV model which doesn't.

Time derivatives are discretized by an implicit Euler scheme. Space discretization is done with the finite element method of order one. To focus on $\epsilon_p(T)$ only, we have chosen a very fine mesh and a very small time step. The numerical solution π, considered as "exact", is projected (π_n) on a reduced basis of size $I = n$ defined as

$$\begin{aligned}
&\text{For BS model by } \omega_i(x) = \omega_i^{BS} := \mathcal{L}^{\sigma_0}[u_{\sigma_i}](x,T) \qquad \forall i = 1,\dots,n\\
&\text{For GV model by } \omega_i(x) = \omega_i^{GV} := \mathcal{L}^{\sigma_{GV}}[u_{\sigma_i}](x,T) \qquad \forall i = 1,\dots,n\\
&\text{For CEV model by } \omega_i(x) = \omega_i^{CEV} := \mathcal{L}^{\sigma_{CEV}}[u_{\sigma_i}](x,T) \qquad \forall i = 1,\dots,n
\end{aligned}$$

and $\epsilon_p(T)$ is computed.

We plot in Fig. 4.1 the results versus the number of basis functions. We observe a good

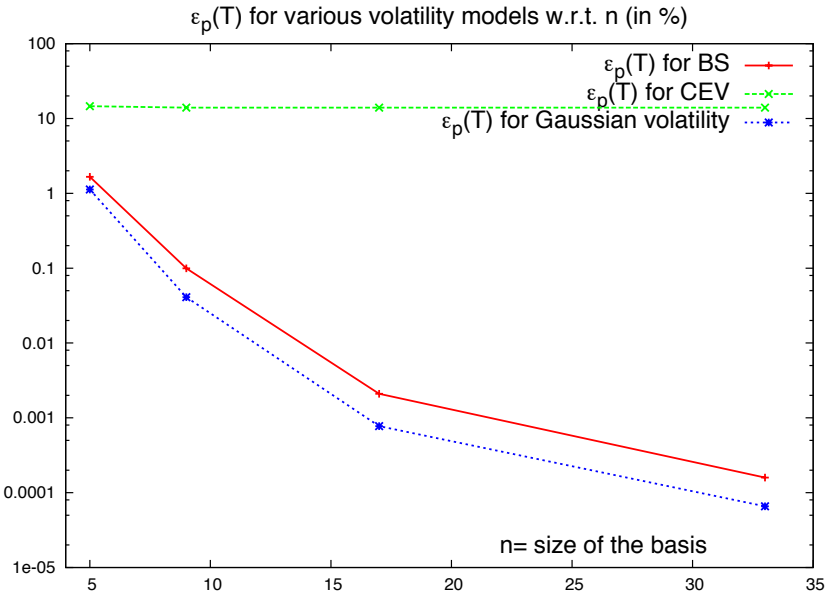

FIG. 4.1. *Relative errors $\epsilon_p(T)$ on $\mathcal{L}^\sigma$ basis only on $\Omega_\epsilon = [28.6, 56]$. The curve for CEV is to be compared with Fig .3.4; it shows that when the symmetry condition is not satisfied the $\omega_i(x) = \omega_i^{CEV}$ are not sufficient.*

convergence behavior for the two symmetric cases and a non decreasing error for the CEV model which does not fulfill the symmetry condition.

4.2. The basis in a special case of CEV model. For the basis presented in (3.6) we can prove the following property:

PROPOSITION 4.5. *For CEV model, $\{\mathcal{L}^{\sigma_0} u_{\sigma_i}\}_i \cup \{\mathcal{L}^{\sigma_{CEV}} u_{\sigma_i}\}_i$ is a basis of the space of C^∞ functions which decay exponentially at infinity.*

Proof. : As seen earlier $\mathcal{L}^{\sigma_0} u_{\sigma_i}$ is proportional to $h_i := \exp(-\frac{x^2}{2\sigma_i^2 T})$.

With the constants σ_i chosen so as to make a basis for the even functions of x which decay exponentially at infinity, let us show that for any β, any fast decaying function at infinity f can be written as

$$f(x) = e^{\frac{x}{2}} \sum_i (a_i + b_i e^{2\beta x}) h_i(x) \tag{4.8}$$

It will prove the proposition because $\{\mathcal{L}^{\sigma_{CEV}} u_{\sigma_i}\}_i$ is proportional to $e^{2\beta x} h_i(x)$ for some appropriate β.

To prove (4.8) let $g(x) = f(x)e^{-\frac{x}{2}}/(e^{2\beta x} - e^{-2\beta x})$. As $g(x) + g(-x)$ is even in the x variable there exist a_i such that

$$g(x) + g(-x) = \sum_i a_i h_i(x)$$

Similarly there exist b_i such that

$$e^{-2\beta x} g(x) + e^{2\beta x} g(-x) = \sum_i b_i h_i(x)$$

By elimination of $g(-x)$ we find

$$(e^{2\beta x} - e^{-2\beta x}) g(x) = e^{2\beta x} \sum_i a_i h_i(x) - \sum_i b_i h_i(x)$$

In terms of f it gives

$$(e^{2\beta x} - e^{-2\beta x}) f(x) e^{-\frac{x}{2}}/(e^{2\beta x} - e^{-2\beta x}) = \sum_i (e^{2\beta x} a_i - b_i) h_i(x)$$

which proves the result. □

4.3. Convergence in a jump-diffusion example. We will now show convergence of the projection on a specific jump-diffusion model.

To prove that $\{\mathcal{L}^\sigma u_{\sigma_i} \cup \mathcal{L}_J u_{\sigma_i}\}_i$ forms a basis of a subspace U of the square integrable functions which decay exponentially fast at infinity, we shall use the property that if $\mathcal{L}$ is continuous and injective from U to $\mathcal{L}U$ and u_i is a basis of U then $\mathcal{L}u_i$ is a basis of $\mathcal{L}U$.

We know from the previous theorem that $\mathcal{L}^\sigma(u_{\sigma_i} - u_\Sigma)$ is a basis for the functions $u \in H^2(\mathbb{R})$, with exponential decay at infinity and such that $u(-x) = e^{-x}u(x)$; therefore, since $(\mathcal{L}^\sigma)^{-1}$ is continuous, $\{u_{\sigma_i} - u_\Sigma\}_{i\in I}$ is a basis for the functions of $H^2(\mathbb{R})$ with exponential decay at infinity and which satisfy the same symmetry condition, because $\mathcal{L}^\sigma$ preserves the condition.

Consequently $\{\mathcal{L}_J(u_{\sigma_i} - u_\Sigma)\}_{i\in I}$ is a basis for the space of functions which satisfy a symmetry condition, which we now proceed to establish.

First we notice that by definition of $\mathcal{L}_J$ and by (2.8) we have

$$J(-z) = e^{-\frac{2\mu z}{\delta^2}} J(z)$$

Hence, with $z' = -z$ and $c = \lambda(e^{\frac{\delta^2}{2}+\mu} - 1)$,

$$\begin{aligned}
\mathcal{L}_J u(-x) &= \int_{\mathbb{R}} u(z-x)J(z)\mathrm{d}z - \lambda u(-x) - c\partial_x u(-x) \\
&= -\int_{\mathbb{R}} u(-z'-x)J(-z')\mathrm{d}z' - \lambda u(-x) - c\partial_x u(-x) \\
&= -e^{-x}[\int_{\mathbb{R}} e^{-z'} u(x+z') e^{-\frac{2\mu}{\delta^2}z'} J(z')\mathrm{d}z' + (\lambda + c)u(x) - c\partial_x u(x)] \qquad (4.9)
\end{aligned}$$

because $u(-x) = e^{-x}u(x)$ implies that $\partial_x u(-x) = e^{-x}(u(x) - \partial_x u(x))$.

If $\mu = -\frac{1}{2}\delta^2$ then

$$\mathcal{L}_J u(-x) + (\lambda + \frac{c}{2})u(-x) = -e^{-x}(\mathcal{L}_J u(x) + (\lambda + \frac{c}{2})u(x))$$

Because this is the complementary condition to $u(-x) = e^{-x}u(x)$, $\{\mathcal{L}^\sigma u_{\sigma_i} \cup \mathcal{L}_J(u_{\sigma_i} - u_\Sigma) + (\lambda + \frac{c}{2})(u_{\sigma_i} - u_\Sigma)\}_i$ is a basis of the whole space.

Indeed let v be any smooth function decaying exponentially fast at infinity. The following identity holds

$$v(x) = \frac{1}{2}\left[v(x) + e^x v(-x)\right] + \frac{1}{2}\left[v(x) - e^x v(-x)\right].$$

It shows that v has been written as a sum of a function verifying the first symmetry condition plus a function verifying the second symmetry condition.

Now $(\lambda+\frac{c}{2})(u_{\sigma_i}-u_\Sigma)$ can be decomposed on the first set of basis functions, so $\{\mathcal{L}^\sigma u_{\sigma_i} \cup \mathcal{L}_J(u_{\sigma_i} - u_\Sigma)\}_i$ is also a basis. Therefore any smooth function v which decays exponentially fast at infinity can be written on that basis. So we have proved the following:

PROPOSITION 4.6. *In a Merton jump-diffusion model with $\mu = -\frac{1}{2}\delta^2$ the pricing function can be decomposed on $\{\mathcal{L}^\sigma u_{\sigma_i} \cup \mathcal{L}_J u_{\sigma_i}\}_i$.*

REMARK 5. *The convergence is exponential for the same reason as in the symmetric case.*

REMARK 6. *When neither σ nor J satisfy the conditions of the last two theorems, still we suspect that we have a basis because the two operators have symmetries that are "complementary". In fact the numerical simulations show convergence even when the conditions of the above theorem are not verified! Note that we could alternatively use $\{\mathcal{L}^\sigma u_{\sigma_i} \cup e^{-\beta x}\mathcal{L}^\sigma u_{\sigma_i}\}_i$, for some $\beta > 0$ as in the case of CEV, but this may not necessarily lead to a sparse representation.*

5. A Galerkin scheme with a reduced basis.

5.1. Galerkin method. The Galerkin method is a general and robust methodology to approximate a partial (integro-) differential equation via its variational formulation. It has already been applied to the PIDE problem (2.6): the reader is refered to [12] and [6] for more details and existence results. If $(\cdot,\cdot)$ denotes the L^2 scalar product on $\mathbb{R}$, one seeks $\pi(\cdot,t) \in H^1(\mathbb{R})$, (the Sobolev space of order 1), solution of

$$\begin{aligned} &\partial_\tau(\pi,\omega) + a^\sigma(\pi,\omega) + (\mathcal{L}_J\pi,\omega) = (f,\omega), \quad \forall\omega \in H^1(\mathbb{R}) \\ &\text{with } a^\sigma(\pi,\omega) = \int_{-\infty}^{+\infty}\left[\tfrac{\sigma^2}{2}\partial_x\pi\partial_x\omega + \left(\sigma\partial_x\sigma + \tfrac{\sigma^2}{2}\right)\partial_x\pi\,\omega\right] \end{aligned} \tag{5.1}$$

A finite number of independent functions $\omega_i \in H^1(\Omega)$ are chosen to generate a subset $H_I \subset H^1(\Omega)$:

$$H_I = \text{Sp}\{\omega_i\}_{i=1,..,I}.$$

and we look for an approximation of $\pi_I \in H_I$ of π :

$$\pi_I(x,\tau) = \sum_{j=1}^{I}\alpha_j(\tau)\omega_j(x)$$

by solving

$$\partial_\tau(\pi_I,\omega_i) + a^\sigma(\pi_I,\omega_i) + (\mathcal{L}_J\pi_I,\omega_i) = (f,\omega_i), \quad \forall i = 1,..,I \tag{5.2}$$

In effect this is a linear system of differential equations of the form

$$\begin{aligned} &M\dot{\alpha}(\tau) + A\alpha(\tau) = F(\tau), \qquad \text{where } \alpha(\tau) = \{\alpha_j(\tau)\}_{j=1,\dots,I} \\ &\text{and } A_{i,j} = a^\sigma(\omega_j,\omega_i) + (\mathcal{L}_J\omega_j,\omega_i) \text{ and with } M_{i,j} = (\omega_j,\omega_i), \quad F_i = (f,\omega_i). \end{aligned}$$

An Euler implicit scheme is used to discretize the time derivative:

$$(M + \delta\tau A)\alpha^{n+1} = M\alpha^n + \delta\tau F^n \tag{5.3}$$

5.2. Numerical Results. We use this scheme to price a call option under the CEV diffusion model and the Merton jump-diffusion model. To study the performance of the method, we use two distinct error metrics, expressed in percentage. The first one is the relative pricing error $\epsilon(S)$. Another appropriate error metric for pricing applications is the relative error $\epsilon_\Sigma(S)$ expressed in term of Black-Scholes (B-S) implied volatility: We define

$$\epsilon(S) = \frac{|u_I(S,0) - u_{Exact}(S,0)|}{|u_{Exact}(S,0)|} \quad \text{and} \quad \epsilon_\Sigma(S) = \frac{|\Sigma_I(S,0) - \Sigma_{Exact}(S,0)|}{|\Sigma_{Exact}(S,0)|} \tag{5.4}$$

where Σ is the implied volatility computed by the inversion of B-S formula with respect to the volatility σ. All the parameters for models are those presented in §3.1.2 . The linear system associated to the Galerkin discretization is solved with a `GMRES` solver.

5.2.1. CEV model. We first present the numerical results obtained for CEV model. In Fig. 5.1, we first plot the relative error $\epsilon(S)$ in option price and then in term of implied volatility (Fig. 5.2 and 5.3). The convergence results are shown in the two tables 5.2.1 and 5.2. We recall that $\Omega_\epsilon = [28.6, 56]$.

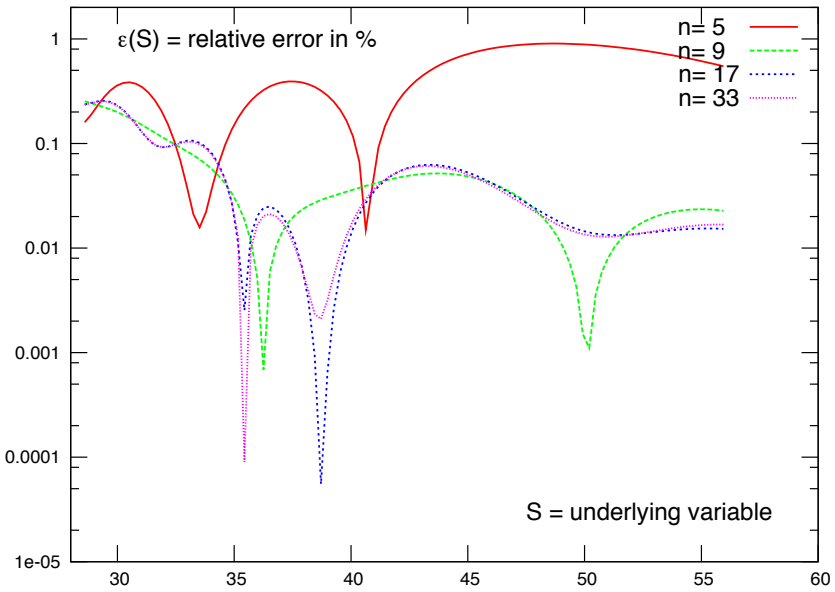

FIG. 5.1. *Pointwise relative error $\epsilon(S)$ (defined in 5.4 and expressed in percentage) for a European call option under CEV's solution with respect to the underlying variable $S \in \Omega_\epsilon$ for different values of n, the number of basis vectors (recall that the total number of vectors is $2n + 1$). The results are plotted in logscale.*

n	I	$C_I(Spot,0)$	$\epsilon(Spot)$	$\|\|\epsilon(S)\|\|_2$	$\|\|\epsilon(S)\|\|_\infty$
5	10	22.584	0.178 %	2.337 %	8.757 %
9	18	11.511	0.036 %	0.078 %	0.254 %
17	34	11.509	0.014 %	0.075 %	0.256 %
33	66	11.509	0.017 %	0.074 %	0.253 %
Exact		11.507			

TABLE 5.1

Relative errors $\epsilon(S)$ for a European call option price under CEV model w.r.t. the size of the basis. The L^2 and L^∞ errors are computed on Ω_ϵ

n	I	$\Sigma_I(Spot,0)$	$\epsilon_\Sigma(Spot)$	$\|\|\epsilon_\Sigma(S)\|\|_2$	$\|\|\epsilon_\Sigma(S)\|\|_\infty$
5	10	0.6703	0.303 %	1.940 %	5.721 %
9	18	0.1515	0.174 %	0.322 %	1.274 %
17	34	0.1514	0.067 %	0.277 %	0.815 %
33	66	0.1514	0.081 %	0.277 %	0.897 %
Exact		0.1513			

TABLE 5.2

Relative errors $\epsilon_\Sigma(S)$ on implied volatility for a European call option under CEV model w.r.t. the size of the basis. The L^2 and L^∞ errors are computed on Ω_ϵ

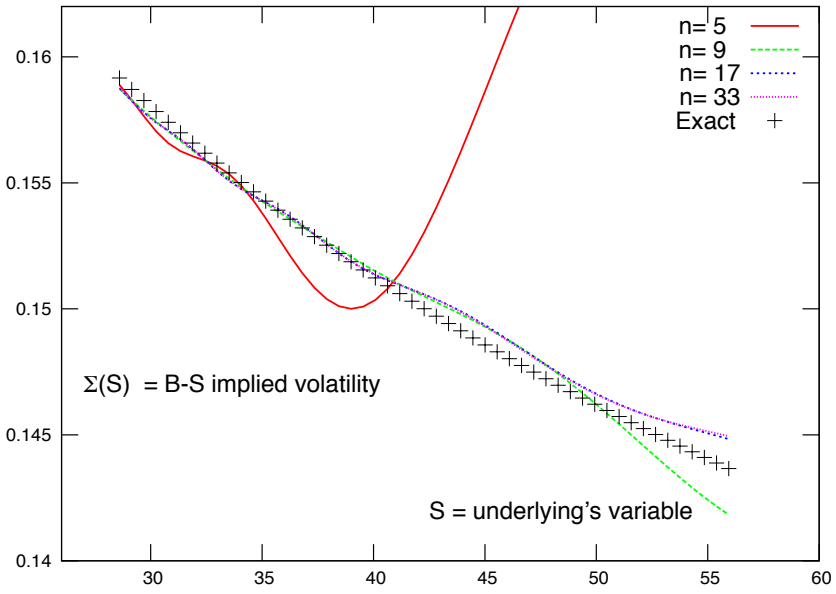

FIG. 5.2. *CEV implied volatility for a European call option w.r.t. the underlying variable $S \in \Omega_\epsilon$ for various size of basis.*

The results show that 18 basis functions (i.e. $n = 9$) are sufficient to reach an acceptable accuracy under both error metrics. The gain obtained by adding more basis functionals is small.

5.2.2. Merton model. For this model, we choose to use the least-square solver `dgelss.c` of LAPACK. We plot in Fig. 5.4, 5.5 and 5.6 and in tables 5.3 and 5.4 the same indicators as

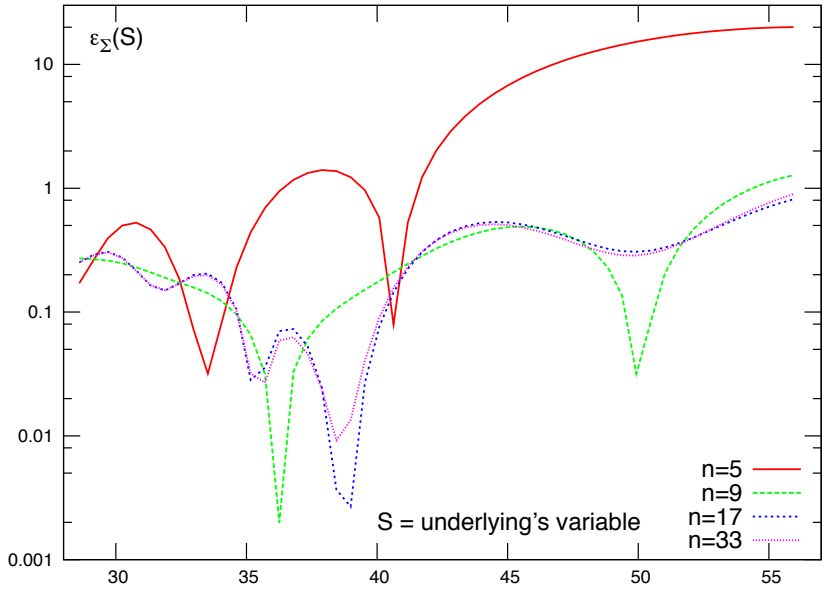

FIG. 5.3. *Relative Error of CEV implied volatility, $\epsilon_\Sigma(S)$ for a European call option w.r.t. the underlying variable $S \in \Omega_\epsilon$ for various size of basis. The results are expressed in percentage and plotted in logscale.*

n	I	$C_h(Spot)$	$\epsilon(Spot)$	$\|\|\epsilon(S)\|\|_2$	$\|\|\epsilon(S)\|\|_\infty$
5	10	22.584	0.178 %	2.337 %	8.757 %
9	18	22.632	0.033 %	0.065 %	0.120 %
17	34	22.625	0.005 %	0.022 %	0.049 %
33	66	22.624	0.003 %	0.018 %	0.032 %
Exact		22.624			

TABLE 5.3

Relative errors $\epsilon(S)$ for a European call option price under Merton model w.r.t. the size of the basis. The L^2 and L^∞ errors are computed on Ω_ϵ

before. We recall $\Omega_\epsilon = [12.6, 127]$

The results obtained for the Merton model are rather good. The basis is efficient and as accurate as a standard finite element method on a refined mesh but at a lower computational cost as the linear system to solve at every time step is much smaller.

5.2.3. Study of the spectrum for Merton model. Here we are interested in the spectrum of the matrix $C = M + \delta\tau A$ of the Galerkin scheme obtained for 66 basis functions (see (5.3) with $\delta\tau = 0.05$).

Figure 5.7 illustrates the exponential decay of the C-matrix eigenvalues (normalized by the trace of the matrix), a key ingredient in the search for a reduced basis as previously explained. Note that the reduction of the decay rate that occurs after the fourtieth eigenvalue

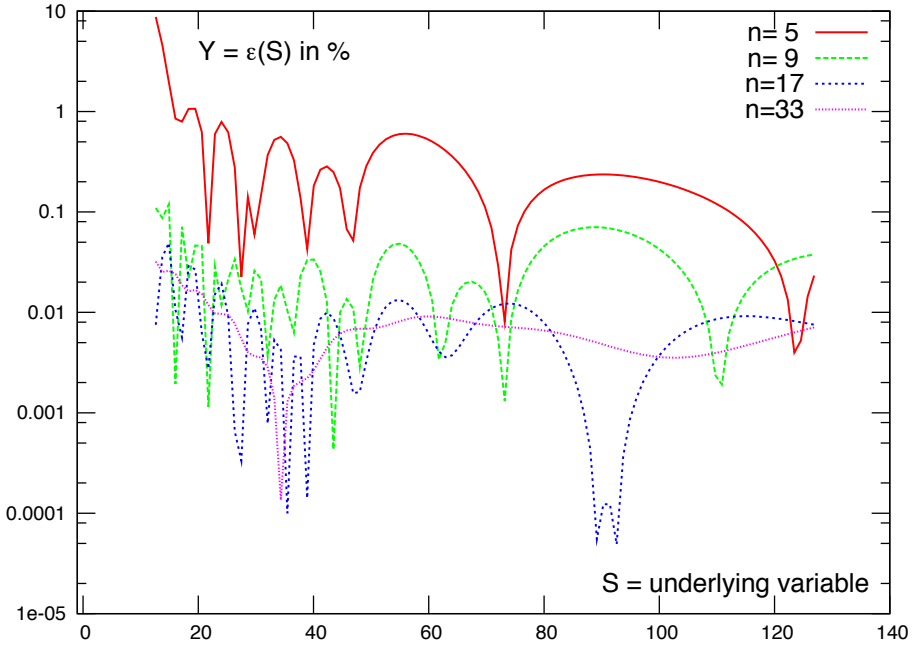

FIG. 5.4. *Pointwise relative error $\epsilon(S)$ (defined in 5.4 and expressed in percentage) for a European call option under Merton solution with respect to the underlying variable $S \in \Omega_\epsilon$. The results are plotted in logscale.*

n	I	$\Sigma_h(Spot)$	$\epsilon_\Sigma(Spot)$	$\|\|\epsilon_\Sigma(S)\|\|_2$	$\|\|\epsilon_\Sigma(S)\|\|_\infty$
5	10	0.6703	0.303 %	1.940 %	5.721 %
9	18	0.6727	0.057 %	0.171 %	0.315 %
17	34	0.6724	0.008 %	0.037 %	0.063 %
33	66	0.6724	0.004 %	0.029 %	0.056 %
Exact		0.6723			

TABLE 5.4

Relative errors $\epsilon_\Sigma(S)$ on implied volatility for a European call option under Merton model w.r.t. the size of the basis. The L^2 and L^∞ errors are computed on Ω_ϵ

is surely due to numerical noise.

In Fig. 5.8 we show the relative error of the Galerkin scheme on the eigenvector basis. We observe that 20 vectors are sufficient to achieve convergence. Moreover the convergence rate is similar to the one observed with the basis w^i, which reinforces confidence in the fact that this basis is good and further reduction is unnecessary.

5.3. Numerical Complexity and Computing Time. If σ is a function of y and τ, it is best to express it on an exponential and/or a polynomial basis; for instance,

$$\sigma(x,t) = \sigma_0 + \sigma_\infty(y^k + \frac{1}{y^k}) + \sum_{j=1}^{Q} \sigma_j(t) e^{-\alpha_j \ln^2 y} \tag{5.5}$$

will lead to a symmetric solution and includes a smile-like polynomial behavior at infin-

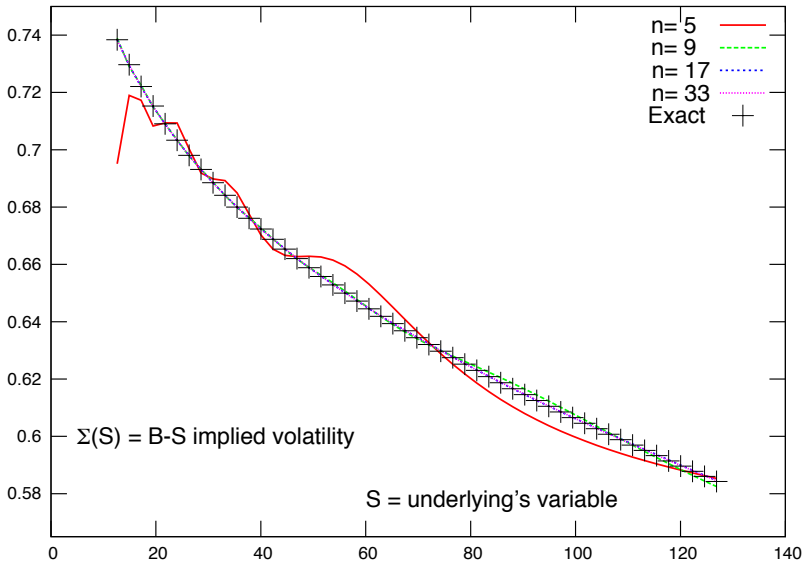

FIG. 5.5. *Merton implied volatility for a European call option w.r.t. the underlying variable* $S \in \Omega_\epsilon$ *for various size of basis.*

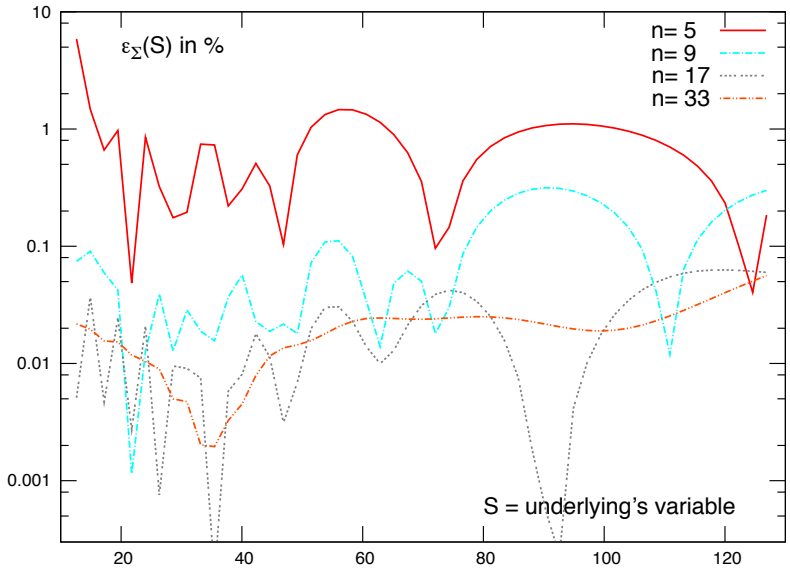

FIG. 5.6. *Relative Error of Merton implied volatility,* $\epsilon_\Sigma(S)$ *for a European call option w.r.t. the underlying variable* $S \in \Omega_\epsilon$ *for various size of basis. The results are expressed in percentage and plotted in logscale.*

ity and zero. Then all integrals can be computed analytically which increases computation speed. Notice that it is fast and not hard to project on (5.5) any volatility symmetric about $y = 1$ and known by a set of point values and find the coefficients $\sigma_j(t)$. Let us show that with such volatilities the reduced basis method is as fast if not faster than the fastest of known methods to compute a call for a general volatility σ, namely the finite difference methods.

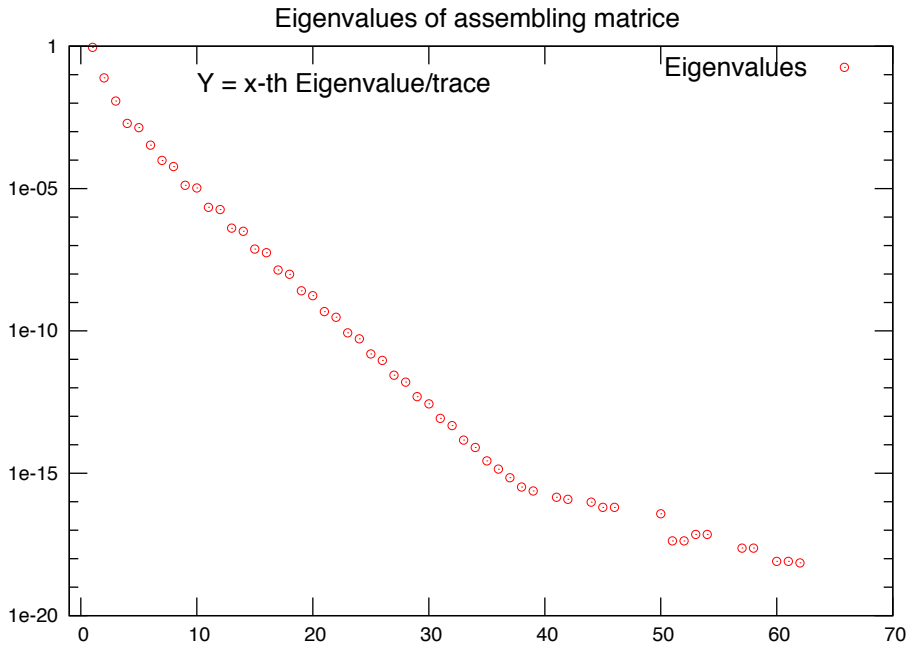

FIG. 5.7. *Eigenvalues of the matrix C normalized by its trace, in log-scale*

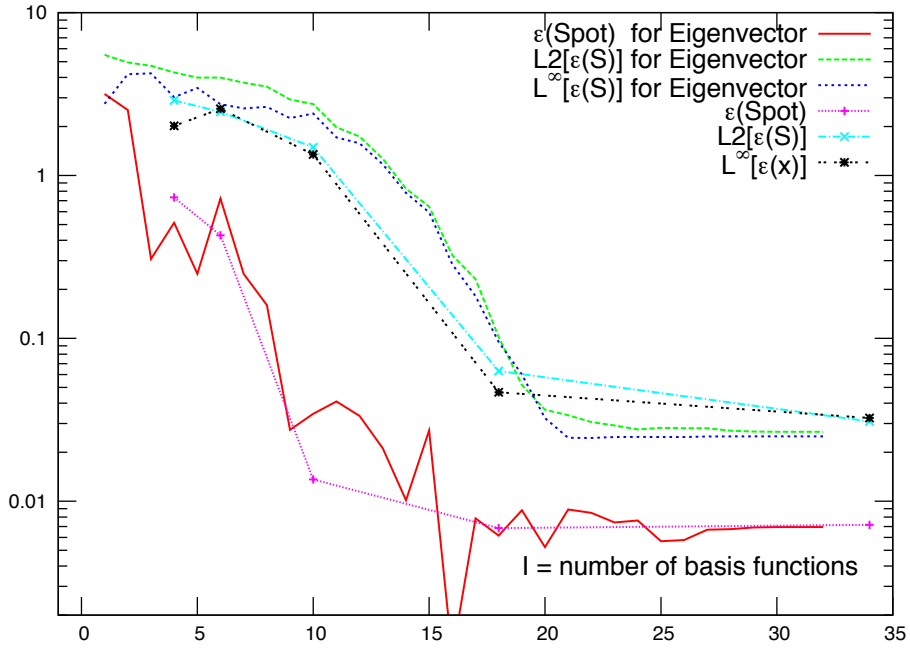

FIG. 5.8. *Relative error in several norms of $\epsilon(S,T)$ in logscale : evolution with the number of eigenvectors in the basis and comparison with the same numbers of w^i vectors in place of eigenvectors.*

If (5.5) is used, then the $Q+2$ matrices are computed once and for all at the cost of $O((Q+2)I^2)$ operations. The linear systems have a rather low condition number (10^{-7} for $I=8$) but they can be solved accurately by LU factorization if $I<15$ beyond which GMRES or SVD must be used. The right hand sides are computed at a cost of $O(I\,Q)$ operations at each time step.

Finally if M is the number of time steps the total number of operations is dominated by the computation of the right hand sides and the resolution of the linear systems $C=(Q\,I+I^3)\,M$. Typically $M\sim I$ and $Q<I$ so $C\sim I^4$. Compare this with a time-implicit finite difference method with M' time steps and $N\sim M'$ mesh points for which the complexity is at best $NM'\sim N^2$. Hence the reduced basis method will be competitive when $I<\sqrt{N}$.

These tests confirm that this method is indeed much faster than the best finite difference/finite element solution of the PDE. Parameters are adjusted so that the precision is 0.5% or less. For instance, an implicit Euler in time finite difference scheme with M'=100 time steps and 200 S-mesh points where the linear system at each iteration is solved by a Gauss factorization – required because σ is time dependent – takes 0.0014" (measured by computing 1000 computations and divide the resulting CPU time by 1000).
On a reduced basis of 10 vectors with implicit time-stepping, the computation takes 0.00018" for $Q=1$. For non-symmetric volatilities I must be doubled but the reduced basis method is still ahead. For jump diffusion PIDE the method is even more competitive because a finite difference scheme usually requires $O(M\,N^2)$ operations, because of the integrals on the right hand sides. With Merton's model and $I=17$ for the same precision, a mesh size of 160 and 200 time steps are needed and the reduced basis method is 6 times faster.

These numbers correspond to computations done on an Intel Core duo 1.86 GHz using only one of the two cores.

6. Application to model calibration. The fact that one can write any call C_σ , solution of the pricing equation (2.1) for a general volatility $\sigma(S,t)$, as

$$C_\sigma(S,t)=C_\Sigma(S,t)+\sum_{i=1}^{I}\alpha_i(t)(C_{\sigma_i}(S,0)-C_\Sigma(S,0)) \tag{6.1}$$

has interesting consequences for calibration.

In general one observes at $t=0$ some calls $\{u_j\}_{j=1}^J$ all based on the same asset S; these have strikes K_j and maturity T_j.

In applications one wishes to choose the function $\sigma(.,.)$ to reproduce these call option prices. The call option, as a function of maturity T and strike K, verifies Dupire's equation [9]:

$$\partial_T u_\sigma-\frac{\sigma^2}{2}\partial_{KK}u_\sigma+r\partial_K u_\sigma=0,\;\; u_\sigma(K,0)=(S-K)^+ \tag{6.2}$$

The structure of this equation is very similar to the backward equation studied above, with a sign change. We may thus use our reduced basis approach for solving it. The calibration problem is an inverse problem for the Dupire equation (6.2). A frequently used method is to

formulate it in terms of an output least squares optimization problem:

$$\sigma = \arg\min_\sigma \sum_{j=1}^{J} |u_\sigma(K_j, T_j) - u_j|^2 \tag{6.3}$$

When a decomposition similar to (6.1) but with K, T as variables, then (6.3) is a sum of independent problems at each time T_j: for each T' one solves

$$\begin{aligned} \alpha(T') = \arg\min_\alpha \sum_{j:T_j=T'} |u(K_j, T'; \alpha) - u_j|^2 \ : \\ u(K_j, T'; \alpha) = u_\Sigma(K_j, T') + \sum_{i=1}^{I} \alpha_i \left[u_{\sigma_i}(K_j, T_M) - u_\Sigma(K_j, T_M)\right] \end{aligned} \tag{6.4}$$

where $T_M = \max T_j$ is the reference time chosen to build the basis. The volatility surface is recovered from Dupire's equation and $u_\sigma(K, T) = u(K, T; \alpha)$; the derivatives with respect to K are computed analytically.

The method is tested on the data shown in Table 6.1 . The rate r is constant: $r = 0.03$. The spot price is 1418.3. In this example there are 6 times T'. The basis is made of Black-Scholes calls with volatility $0.3/\sqrt{i}$, i=2..9. The Black-Scholes solution used for the translation corresponds to $\Sigma = 0.3$. At each T' a set of 8 α_i is computed by solving (6.4) by a conjugate gradient method with a maximum of 300 iterations. We found the optimization more efficient if α_i is replaced by $10 \sin \alpha_i$; this prevents large values. Results are shown in Figure 6.1.

The method is even faster than fitting an implied volatility, but it gives the local volatility only at the times corresponding to the maturity of an observation. The method seems stable and accurate. Restrictions on α such as $\alpha \in (0, 1)$ can be applied for more stability but it may deteriorate the accuracy.

7. Conclusion. We have presented a reduced basis method for solving partial integro-differential equations which arise in option pricing. Our basis functions are constructed in term of solutions to the Black-Scholes equation; their analytical tractability allows for efficient numerical computations and their qualitative properties match those of the solutions in more complex models, yielding correct asymptotic behavior without further effort.

Convergence has been proved for general scalar diffusion models and for special cases of jump diffusion models, with exponential convergence for models verifying a symmetry condition. The numerical tests confirm the accuracy and the efficiency of this reduced basis in the sense that it performs better than, for instance, numerical construction of a reduced basis by SVD techniques. Less than twenty basis functions are usually sufficient to efficiently solve the problems. The method is much faster than finite difference schemes for the Black-Scholes PDE or PIDE. For large number of basis functions, the resulting linear systems may be ill conditioned; fortunately, precision levels sufficient for applications in finance are attained well before this threshold is reached. A deeper analysis would require a posteriori estimates to fix the number of basis functions.

REFERENCES

[1] YVES ACHDOU AND OLIVIER PIRONNEAU, *Computational methods for option pricing*. Vol. 30, Frontiers in Applied Mathematics, SIAM, 2005.

Strike	1 Month	2 Months	6 Months	12 Months	24 Months	36 Months
700						733
800						650.6
900						569.8
1000					467.8	
1100					385.3	
1150					345.4	
1175			265.2			
1200			242	266.1	306.6	
1215				253.4		
1225			219	245		
1250			196.6	224.2	269.2	
1275			174.5	203.9	251	
1300			152.9	184.1	233.2	
1325			131.9	164.9	215.8	
1350			111.7	146.3	198.9	
1365			100			
1375	50.6	60	92.5	139	182.6	
1380	46.1	55.8				
1385	41.8	51.8				
1390	37.5	47.9				
1395	33.4	44				
1400	29.4	40.3	74.5	128.4	166.7	215.9
1405	25.6	36.7				
1410	21.9	33.2				
1415	18.7	29.8				
1420	15.4	26.6				
1425	12.7	23.8	58	111.4	151.5	
1430	10	20.7				
1435	8	18.2				
1440	6.3	15.7				
1445	4.4	13.4				
1450	3.1	11.3	43.3	95.2	136.9	187.5
1455	2.05	9.6				
1460	1.45	7.9				
1475			30.6	80.2		
1500			20.3	54	109.6	160.8
1525			12.6	42.7		
1550			7.5	33		
1575				24.7		
1600			1.95	18.2	64.5	113,9
1700					32.7	75,7
1800					15.5	
1900					5.2	

TABLE 6.1
The prices of a family of calls on the same asset (Eurostoxx50)

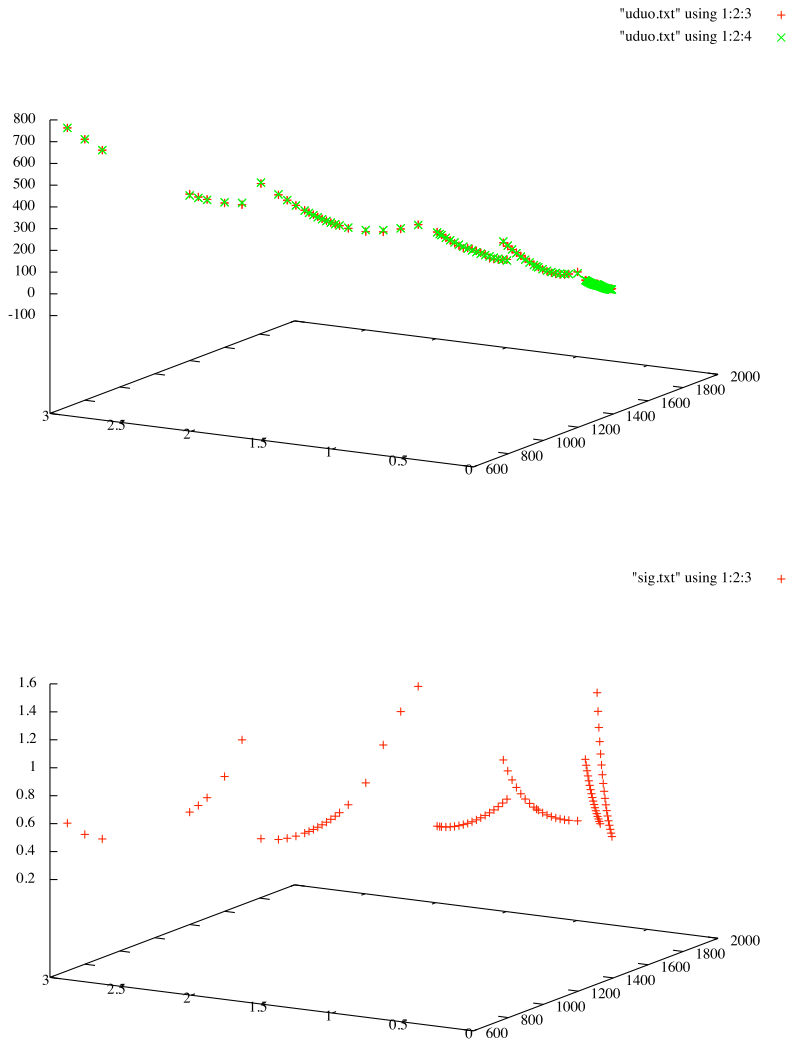

FIG. 6.1. *Top: Observed prices and model predictions for the calls at the observation points; errors are hardly visible (between 1 and 9$) is 4$ at each point on the average. Bottom: the local volatility recovered from the Dupire equation at the observed points. For both graphs the horizontal axis is time, the vertical axis is the price of calls and the other axis is the strike.*

[2] AMEL BENTATA AND RAMA CONT, *Forward equations for option prices in semimartingale models*, forthcoming in Finance & Stochastics, 2009.
[3] LEIF ANDERSEN AND JESPER ANDREASEN, *Jump diffusion models: Volatility smile fitting and numerical methods for pricing*, Review of Derivatives Research, 4 (2000), pp. 231–262.
[4] DAMIANO BRIGO & FABIO MERCURIO (2002) *Lognormal mixture dynamics and calibration to market volatility smiles*, International Journal of Theoretical and Applied Finance, Vol. 5, No. 4, 427–446.
[5] PETER CARR AND DILIP B. MADAN *Option valuation using the fast Fourier transform*, J. Comput. Finance,

61–73, 2,1998.
[6] RAMA CONT AND PETER TANKOV *Financial modelling with jump processes*, Chapman and Hall, 2003.
[7] RAMA CONT AND EKATERINA VOLTCHKOVA, *A finite difference scheme for option pricing in jump diffusion and exponential Lévy models*, SIAM J. Numer. Anal., Vol 43, **4**, 1596–1626, 2005.
[8] JOHN COX *Notes on option pricing I: Constant Elasticity of Variance diffusions*, Working Paper Stanford University, 1975.
[9] BRUNO DUPIRE, *Pricing and hedging with smiles*, in Mathematics of Derivative Securities, M. Dempster and S. Pliska, eds., Cambridge University Press, 1997, pp. 103–111.
[10] PAUL GLASSERMAN, *Monte Carlo Methods in Financial Engineering*, Series: Stochastic Modelling and Applied Probability , Vol. 53, 2003.
[11] ALAN LEWIS *A simple option formula for general jump-diffusion and other exponential Lévy processes.* available from `http://www.optioncity.net`, 2001
[12] ANA-MARIA MATACHE, TOBIAS VON PETERSDOFF AND CHRISTOPH SCHWAB, *Fast deterministic pricing of Lévy driven assets*, J.Mathematical Modelling and Numerical Analysis, Vol.38, **1**, 37–72, 2004.
[13] ROBERT C. MERTON *Option pricing when underlying stock returns are discontinuous*, J. Financ. Econ., Vol.3, 125–144, 1976.
[14] OLIVIER PIRONNEAU *Calibration of options on a reduced basis*, Journal of Computational and Applied Mathematics, Vol. 232, **1**, 139–147, 2009.
[15] W.H. PRESS, S.A. TEUKOLSKY, W.T. VETTERLING AND B.P. FLANNERY Numerical Recipes in C, 2nd edition, Cambridge University Press, 1992.
[16] EKKEHARD W. SACHS AND MATTHIAS SCHU *Reduced Order Models (POD) for calibration Problems in Finance*, Proceedings of ENUMATH 2007, 361–368, 2008.
[17] MARK SCHRODER *Computing the Constant Elasticity of Variance option pricing formula*, J. of Finance, Vol. 44, **1**, 211-219, 1989.

Appendix A: proof of Proposition 3.1. With the log forward moneyness variable x, the probability density function under the Black-Scholes model is: $\rho_\tau(x) = \frac{1}{\sqrt{2\pi}\sigma\sqrt{\tau}} e^{-\frac{1}{2\sigma^2\tau}\left(x+\frac{\sigma^2\tau}{2}\right)^2}$

and we introduce $v = \sigma\sqrt{\tau}$

$$\begin{aligned}\omega^J(x) := \mathcal{L}_J[u_\sigma](x,v) &= \int_{\mathbb{R}} [u_\sigma(x+z,v) - u_\sigma(x,v) - (e^z-1)\partial_x u_\sigma(x,v)]J(z)dz \\ &= \int_{\mathbb{R}} u_\sigma(x+z,v)J(z)dz - \lambda u_\sigma(x,v) - \lambda(e^{\frac{\delta^2}{2}+\mu}-1)\partial_x u_\sigma(x,v)\end{aligned}$$

We note $\gamma = x+z+s$ and $X = x - \frac{\sigma^2\tau}{2}$

$$\begin{aligned}\int_{\mathbb{R}} u_\sigma(x+z,v)J(z)dz &= \int_{\mathbb{R}}\int_{\mathbb{R}} \left(e^{x+z+s}-1\right)^+ \rho_\tau(s)dsk(z)dz \\ &= \int_{\mathbb{R}} (e^\gamma - 1)^+ \left[\int_{\mathbb{R}} \rho_\tau(\gamma-(x+z))k(z)dz\right] d\gamma \\ &= \frac{\lambda}{\sqrt{2(\delta^2+v^2)\pi}} \int_0^\infty (e^\gamma - 1)\, e^{-\frac{1}{2[\delta^2+v^2]}[\gamma-X-\mu]^2} d\gamma \\ &= \lambda\left[e^{x+\mu+\frac{\delta^2}{2}}\mathcal{N}\left(\frac{x+\mu+\delta^2+\frac{v^2}{2}}{\sqrt{\delta^2+v^2}}\right) - \mathcal{I}\left(\frac{x+\mu-\frac{v^2}{2}}{\sqrt{\delta^2+v^2}}\right)\right]\end{aligned}$$

Appendix B: Study of the spectrum of $\mathcal{L}^\sigma$. By definition, w^i, scaled so as to have a L^2 norm equal to 1, is:

$$w^i = \frac{\exp(-\frac{1}{4}(\frac{x}{v_i}-v_i)^2)}{\sqrt{2\sqrt{2\pi}v_i}}, \text{ with } v_i = \sqrt{\frac{\sigma_i^2 T}{2}} \text{ because } \int_{\mathbb{R}} e^{-\frac{y^2}{2}}\mathrm{d}y = 2\sqrt{2\pi}$$

When $v_i = i^{-\frac{1}{2}}$ with some algebra one finds that

$$(w^i, w^j) = \sqrt{\frac{v_i v_j}{2(v_i^2+v_j^2)}}\exp(-\frac{1}{4}\frac{(v_i^2-v_j^2)^2}{v_i^2+v_j^2}) = \sqrt{\frac{\sqrt{ij}}{\sqrt{2}(i+j)}}\exp(-\frac{1}{4}\frac{(i-j)^2}{ij(i+j)})$$

We need to establish similar expressions for $(\partial_x w^i, w^j)$ and $(\partial_x w^i, \partial_x w^j)$.

$$(\partial_x w^i, w^j) = \sqrt{\frac{v_i v_j}{2(v_i^2+v_j^2)}}\exp(-\frac{1}{4}\frac{(v_i^2-v_j^2)^2}{v_i^2+v_j^2})\frac{v_j^2-v_i^2}{2(v_i^2+v_j^2)} = (w^i,w^j)\frac{i-j}{2(i+j)}$$

$$\begin{aligned}(\partial_x w^i, \partial_x w^j) = \sqrt{\frac{v_i v_j}{16\pi(v_i^2+v_j^2)}}&\exp(-\frac{1}{4}\frac{(v_i^2-v_j^2)^2}{v_i^2+v_j^2}) \\ &\frac{a^2}{v_i v_j}[\int_{\mathbb{R}} y^2 e^{-\frac{y^2}{4}}\mathrm{d}y + (2a-\frac{v_i^2}{a})(2a-\frac{v_j^2}{a})\int_{\mathbb{R}} e^{-\frac{y^2}{4}}\mathrm{d}y] \\ &= (w^i,w^j)\frac{v_i v_j}{v_i^2+v_j^2}(2-\frac{(v_i^2-v_j^2)^2}{v_i^2+v_j^2}) \\ &= (w^i,w^j)\frac{\sqrt{ij}}{i+j}(2-\frac{(i-j)^2}{ij(i+j)})\end{aligned}$$

The variational form of the problem leads to the linear system for the vector $\alpha(t)$:

$$B\dot{\alpha} + \frac{\sigma^2}{2}A\alpha = B\tilde{f}$$

where $B_{ij} = (w^i, w^j),\ A_{ij} = (\partial_x w^i, \partial_x w^j) + (w^i, \partial_x w^j)$ and $\tilde{f}_i$ is the component on w^i of the right hand side, i.e. $f(x,t) = \sum \tilde{f}_i(t) w^i(x)$.

The following tables display the first eigenvalues of A,B and A with respect to B for different values of n, the number of σ-basis functions.

Notice the rapid decay of the eigenvalues of A and the rapid growth of those of B.

2.8874	5.6688	8.4913	11.3288
0.5872	1.1587	1.6717	2.1722
0.05843	0.2167	0.3736	0.5175
0.002407	0.02506	0.06279	0.1076
0.00003339	0.001685	0.006536	0.01421
	0.00007929	0.00052435	0.001498
	0.000002448	0.00003150	0.0001236
	0.00000005106	0.0000015210	0.000008636
	0.0000000008225	0.00000005600	0.0000004925
	−0.0000000002322	0.000000001366	0.00000002433
		−0.0000000009870	−0.000000001522
		−0.0000000001615	0.000000001300

First 12 eigenvalues of the matrix $A = ((\mathcal{L}^\sigma w^i, w^j))$ for $n = 5, 10, 15, 20$ when $\sigma^2 T = 2$

		0.0000000001159
		0.0000000005094
	−0.0000000007761	0.0000000009339
	-6.630×10^{-11}	0.000000003368
	0.000000003418	0.0000001086
	0.0000001979	0.000002650
	0.000007586	0.00005220
0.000003812	0.0002038	0.0008265
0.0003502	0.003919	0.01037
0.01271	0.05291	0.09952
0.2203	0.4838	0.7257
3.3020	6.530	9.7701

Last 12 eigenvalues of the matrix $B = ((w^i, w^j))$ for $n = 5, 10, 15$

$$\begin{bmatrix} 9.1544 + 0.9648\,i \\ 9.1544 - 0.9648\,i \\ 0.8117 \\ 4.1003 \\ 2.2851 \end{bmatrix} \quad \begin{bmatrix} 16.4818 + 3.1441\,i \\ 16.4818 - 3.1441\,i \\ 9.7760 + 1.665\,i \\ 9.7760 - 1.6652\,i \\ 5.2870 + 0.7487\,i \\ 5.2870 - 0.7487\,i \\ 3.53077 \\ 0.7664 + 0.1090\,i \\ 0.7664 - 0.1090\,i \\ 1.7905 \end{bmatrix} \quad \begin{bmatrix} 20.6981 + 4.2722\,i \\ 20.6981 - 4.2722\,i \\ 12.8389 + 3.2087\,i \\ 12.8389 - 3.2087\,i \\ 0.7675 \\ 0.5482 \\ 1.5402 \\ 7.9943 + 1.9323\,i \\ 7.9943 - 1.9323\,i \\ 1.7395 \\ 2.6983 \\ 4.1079 + .3209\,i \end{bmatrix}$$

First 12 eigenvalues of $B^{-1}A = ((w^i, w^j))^{-1}((\mathcal{L}^\sigma w^i, w^j))$ for $n = 5, 10, 15,\ \sigma^2 T = 2$

These computations where done with the following `Maple9` program:

```
n:=5;
M:=matrix(n,n,(i,j)->sqrt(sqrt(i*j)/(i+j))*exp(-(i-j)^2/(4*i*j*(i+j))));
I:=matrix(n,n,(i,j)->sqrt(sqrt(i*j)/(i+j))*exp(-(i-j)^2/(4*i*j*(i+j)))*
          ((i-j)/(i+j)/2 + sqrt(i*j)*(2-(i-j)^2/((i+j)*i*j))/(i+j)));
evalf(Eigenvals(I,M,vects));print(vects);vects:='vects';
evalf(Eigenvals(I,vects));print(vects);vects:='vects';
evalf(Eigenvals(M,vects));print(vects);vects:='vects';
```